


SPE/ISRM 78213

# Geomechanical Fault Characterization: Impact on Quantitative Fault Seal Risking

Richard M. Jones (Woodside Energy), David N. Dewhurst SPE (CSIRO Petroleum), Richard R. Hillis SPE (NCPGG, University of Adelaide) and Mildren, S. D. SPE (NCPGG, University of Adelaide).

Copyright 2002, Society of Petroleum Engineers Inc.

This paper was prepared for presentation at the SPE/ISRM Rock Mechanics Conference held in Irving, Texas, 20-23 October 2002.

This paper was selected for presentation by an SPE/ISRM Program Committee following review of information contained in an abstract submitted by the author(s). Contents of the paper, as presented, have not been reviewed by the Society of Petroleum Engineers or International Society of Rock Mechanics and are subject to correction by the author(s). The material, as presented, does not necessarily reflect any position of the Society of Petroleum Engineers, International Society of Rock Mechanics, its officers, or members. Papers presented at SPE/ISRM meetings are subject to publication review by Editorial Committees of the Society of Petroleum Engineers. Electronic reproduction, distribution, or storage of any part of this paper for commercial purposes without the written consent of the Society of Petroleum Engineers is prohibited. Permission to reproduce in print is restricted to an abstract of not more than 300 words; illustrations may not be copied. The abstract must contain conspicuous acknowledgment of where and by whom the paper was presented. Write Librarian, SPE, P.O. Box 833836, Richardson, TX 75083-3836, U.S.A., fax 01-972-952-9435.

## Abstract

Fault sealing is one of the key factors controlling hydrocarbon accumulations and can be a significant influence on reservoir behavior during production. Fault seal is, therefore, a major exploration and production uncertainty that requires a rigid, systematic framework within which to quantify the geological risk of trapping hydrocarbons. One of the key uncertainties in this risking procedure is the breaching of structurally bound traps due to the formation of structural permeability networks. Considering a population of faults and fractures, those that are critically stressed are more prone to act as conduits for fluid transmission. Evaluation and mapping of fault seal breach through such networks involves integration of in-situ stress conditions, pore pressure, fault architecture and fault geomechanics.

Geomechanical characterization of well-lithified fault rocks from the Otway Basin and the Northwest Shelf demonstrates that faults can exhibit significant cohesive strength and that fault reactivation and trap breach is influenced by the development of shear, tensile and mixed-mode fractures. The mechanics of the reactivation process are influenced by grain strength and fault morphology. Mercury injection capillary pressures of cataclastic faults indicate a seal capacity of 2400 psi. Following reactivation, seal capacity is reduced ~95% due to the development of a highly connected fracture network. The tensile strength of such healed faults allows failure to occur by shear, tensile and mixed mode fracturing. These data suggest simple application of Byerlee's Law may not always be applicable when predicting reactivation induced fault seal failure. Consequently, geomechanical tools used to predict trap breach via reactivation that assume cohesionless frictional failure are likely to significantly underestimate seal reactivation risk.

The impact of structurally risking traps using Byerlee and laboratory-derived fault data is demonstrated using the Fault Seal Risk Web approach. Application of geomechanical fault data results in a significant reappraisal of prospect structural risk due to consideration of fault healing.

## Introduction

Hydrocarbon exploration and production strategies all involve an element of risk. As with any investment strategy it is the goal of the venture capitalist to minimize this risk. Geological risk minimization begins within a focused evaluation as to the chance of success, i.e. determining the likelihood that all elements of the petroleum system required for economically viable volumes of hydrocarbons to be trapped and developed have been satisfied. The presence of a sealed trap is one of the key factors in the evaluation of geological risk[1,2,3]. A seal is a barrier to the migration of hydrocarbons, either vertically to shallower strata or laterally across faults. According to the mechanism of failure, seals can be considered membrane or hydraulic[4]. Figure 1 illustrates the classification of seal by geometric type and process.

Faults seal if they juxtapose reservoir rocks against sealing rocks[5,6,7]. Fault planes themselves seal if the faulting process has generated a membrane seal, for example by cataclasis[8], cementation/diagenesis[9], framework grain-clay mixing[9] or clay smearing[10]. However, juxtaposition or deformation process seals may be breached if the fault is reactivated subsequent to hydrocarbons charging the trap. It is not necessary for both juxtaposition and deformation process seals to be developed in order for a fault to be sealing. If throw on the fault juxtaposes sealing rocks against reservoir rocks, no deformation process seal is required. Conversely, faults can seal where there is sand/sand juxtaposition across the fault plane and cataclastic processes have reduced pore throat sizes such that the fault zone itself acts as a membrane seal.

Fault sealing due to juxtaposition and deformation processes has received considerable attention, and techniques for the analysis of such (e.g. Allan diagrams, juxtaposition diagrams and shale smear algorithms) are widely applied. However, the risk of seal breach due to reactivation, although recognized[12], has received somewhat less attention. Seal

breach due to fault reactivation has been recognized as a critical risk in the Australian context. For example, in the Timor Sea region, Neogene reactivation related to collision between the Australian and SE Asian plates has breached many Jurassic or older palaeo-traps[13]. Microstructural evidence for cataclasite reactivation in the Otway Basin has also been presented[11].

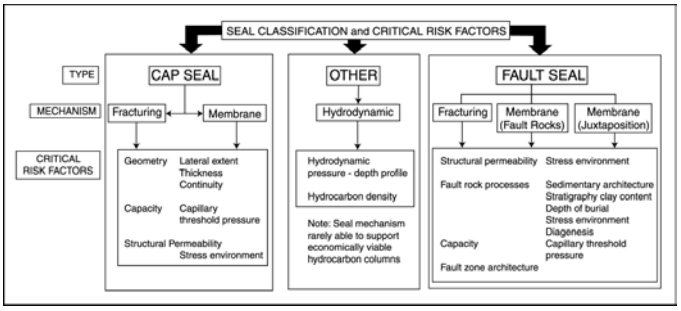


**Figure 1: Seal classification and critical risk factors [11].**

Fault rock microstructural and geomechanical properties are an integrated product of factors such as strain rate, principal stress orientation, shear sense, pore pressure, lithification state and diagenesis. Since mechanical properties change between cohesionless, unlithified sand and brittle cemented sandstones, deformation processes and fault rock products also change. Therefore, it is essential to establish the diagenetic history as well as the burial depth at which the deformation occurred in order to predict fault rock properties. While there are considerable amounts of data available for geomechanical properties of cohesionless slip planes, very little data exists documenting failure conditions for intact fault rocks.

The lack of geomechanical data for naturally occurring intact fault rocks introduces significant uncertainty when assessing the likelihood of fault reactivation and seal breach. This uncertainty is carried into the prospect risking stage via the tenet that a fault seals if deformation processes have created an effective membrane seal ***or*** if displacement juxtaposes sealing rocks against reservoir rocks, ***and*** the fault has not been reactivated subsequent to hydrocarbons charging the trap. This paper thus presents failure envelopes for microstructurally and petrophysically characterized fault rocks sourced from cores in the Carnarvon and Otway Basins of Australia. Further, given that cohesionless friction relations do not describe the failure of these fault rocks, an alternative approach to assessing the risk of fault reactivation and associated seal breach is presented. We also consider a scenario from the Carnarvon Basin where the fault rock is considerably stronger than the surrounding reservoir sandstone. The risking impact of these findings is demonstrated via the integrated fault seal risk expression (FS).

## Integrating geomechanics and fault seal risking

It can be demonstrated that the integrated probability of a fault sealing (FS) can be expressed as:

$$FS = \{1 - [( 1 - a )( 1 - b ) ] \} \times ( 1 - c) \quad (1)$$

where *a, b* and *c* are respectively, the probabilities of deformation process sealing, juxtaposition sealing, and of the fault not being reactivated subsequent to the trap being charged with hydrocarbons. A full discussion of fault seal risking methodology is beyond the scope of this publication. However, for a detailed review of fault seal risking the reader is referred to references 14 and 15.

The three factors influencing fault sealing are assumed to be independent (the probability of independent events occurring is the product of their individual probabilities). In order to combine the probabilities of juxtaposition and deformation process sealing, the probability of neither providing a seal should be considered. The Fault Seal Risk Web illustrates the integrated, multi-parameter approach required for robust fault seal risking and presents an example of probability against seal condition (Figure 2). The seal condition scale is analogous to industry standard probability scales yet with the recognition that a seal condition value of 0.5 does not reflect an equivocal probability of sealing. Under this scheme a risk value of 0.5 is interpreted to reflect an intermediate chance of sealing hydrocarbons.

The FS parameter *c* normalizes the combined probability of membrane and juxtaposition sealing by the likelihood of reactivation. Hence, a trap with a high probability of reactivation would exhibit a low integrated fault seal probability, even if the probability of juxtaposition and membrane sealing were extremely high. Hydrocarbon traps associated with active faults and fractures are riskier than those associated with inactive faults because of the potential for fault-valve activity[16]. Reactivation can breach fault-bound traps even if there is juxtaposition and/or membrane-related seal. The likelihood of reactivation can be assessed given knowledge of the stress field, fault orientation and the failure envelope for the fault rocks. The relationship between these variables also dictates the likely mode of fault failure.

The development of cohesive strength through fault healing allows fault rocks to fail by tensile, shear or mixed mode fracturing. Assuming faults are cohesionless considers only shear failure. A number of recent studies[17,18,19] of the relationship between stresses and fault reactivation/permeability assume that the failure envelopes for fault rocks are described by a cohesionless friction law. However, frictional sliding experiments on cohesionless joints or saw-cuts through rocks of the type summarized by Byerlee[20] do not accurately describe the failure envelopes for faults such as cemented cataclasites that may exhibit significant cohesive strength.

| PROBABILITY | SEAL CONDITION |
|---|---|
| 1 | Certain |
| 0.9 | Extremely likely |
| 0.8 | Very Likely |
| 0.7 | Likely |
| 0.6 | Moderately likely |
| 0.5 | Intermediate |
| 0.4 | Moderately unlikely |
| 0.3 | Unlikely |
| 0.2 | Very unlikely |
| 0.1 | Extremely unlikely |
| 0 | Impossible |

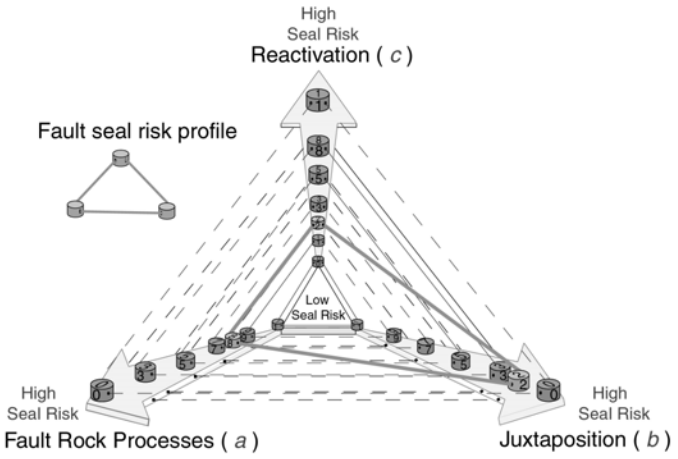


$\{ 1 - [ (1 - a) \times (1 - b) ] \} \times (1 - c) =$ fault seal probability

$a$ = likelihood of fault rock process seal,
$b$ = likelihood of juxtaposition seal, $c$ = likelihood of fault reactivation

**Figure 2: Fault Seal Risk Web and seal condition scale.**

## Geomechanical Testing

Samples of 50 mm length and 25 mm diameter were deformed undrained in a standard triaxial cell with full independent control of cell pressure, pore pressure and axial load. Samples were fully saturated with light oil to avoid damaging clays. Due to the small amounts of samples available, multi-stage triaxial tests were run. Samples were deformed to within a few MPa of peak strength (5-10%) at a set confining pressure then unloaded. Confining pressure was then increased followed by further application of axial load until again close to failure. This cycle was repeated until the desired number of steps had been reached. The final cycle was then taken through to failure and residual strength. Cores of both fault rocks and associated reservoir sandstones were tested for comparative purposes. Where damage zone faults or deformation features were present as single strands, they were oriented at 30° to $\sigma_1$ in the triaxial rig, in the optimum orientation for failure.

## Microstructure

Otway Basin faults analysed during this study were sampled from Jacaranda Ridge-1 and Banyula-1 cores. Fault types include cemented disaggregation zones and phyllosilicate framework fault rocks[21]. Both fault rock types are hosted within competent medium to fine-grained cemented sandstones. Northwest Shelf faults sampled cores recovered from the Echo/Yodel gas condensate field located on the Rankin Trend in the Dampier sub-Basin. Coring of the reservoir intersected sub-seismic faults at a density indicative of inner damage zone architecture.

Cemented disaggregation zone faults from Jacaranda Ridge-1 show parallel and conjugate sets of cemented faults 1-2 mm wide with spacings in the order of 1-4 cm. Phyllosilicate framework faults occur in more argillaceous strata with evidence of clay entrainment into the fault gouge[21]. Faults in Banyula-1 are cemented cataclasites[21]. Slip indicators and displacement magnitudes are readily observed from the disruption of organic laminae and via the entrainment of ankerite into fault zones. Ankerite can form early in the diagenetic sequence and its inclusion within fault gouge, together with a lack of grain fracturing, suggests deformation occurred early in the reservoir burial history under low effective vertical stress. Phyllosilicate framework faults contain sub-parallel anastomosing phyllosilicates seams that isolate pods of deformed and undeformed sandstone. Porosity in the sandstone is occluded by clays. Fracturing of quartz grains is evident and thin clay coats often line boundaries between more rigid quartz grains[21]. These have aided stylolitization in quartz and enhanced cementation and rock strength. Cataclasites recovered from Banyula-1 exhibit a highly heterogeneous fabric with framework grains typically displaying an angular morphology due to fracturing. Post deformation quartz cementation is extensive. Threshold pressures determined by mercury porosimetry for these samples were of the order of 2000-2500 psi (~80-100m gas column).

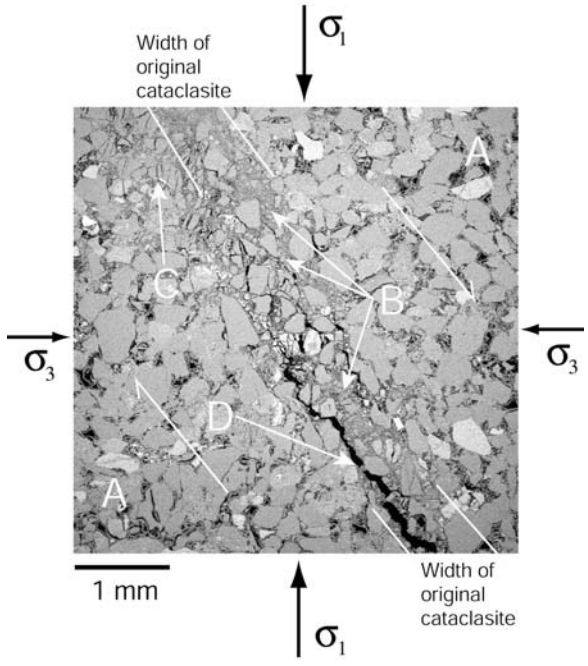


**Figure 3: Backscattered electron micrograph of experimentally reactivated cataclasite (Banyula-1).**

Following experimental reactivation, the Banyula-1 cataclasite microstructure is characterized by a 1-2 mm zone of intense fracturing and granulation (Figure 3). The boundaries of the pre-existing faults retain their primary form and are sharp.

Little deformation resulting from experimental reactivation is noted at distances of tens of microns outside this zone. Hairline fractures crosscut most framework grains within the reactivated fault gouge and a number of large dilatant fractures (apertures of 10-50 μm) are present. These dilatant fractures run parallel to the original fault boundary and are acutely oriented (~30°) to the $\sigma_1$ direction (Figure 3). Reactivation has also resulted in a relatively consistent, sub-vertical fracture orientation sub-parallel to the $\sigma_1$ orientation (Figure 3). These fractures are occasionally linked via subsidiary sub-horizontal fractures. Low angle shear displacement fractures appear to have originated at grain contact points resulting in patches of highly random fracture orientations. Fracturing is most intense along the cataclasite-reservoir boundary. These fractures are interpreted to form networks akin to a structural permeability mesh in which shear and tensile fractures form interlinked networks[22]. Fracturing is generally limited to the largest quartz and feldspar grains. Fine-grained quartz within the original cataclasite generally appears to be unfractured.

Faults within the Yodel-2 core are well-lithified and cemented[21] (Figure 4). The undeformed medium to coarse-grained host sandstone is friable due to only partial quartz and kaolinite cementation. Small faults (1-3 mm gouge width) are noted on both sides of the inner damage zone up to at least 15m in distance (maximum core length) from the principal slip plane. The variation in sandstone grain size over the 30m core length gives rise to varied fault width and geometry. Where little grain size variation occurs faults are single strands of constant width. Where grain size has a greater range, fault traces refract through the interface and are thinner where grain size is finer. The microstructure of the principal fault recovered by Yodel-2 core is complex and can be divided into two distinct domains[21]. The inner fault gouge is heavily cemented by pyrite and is composed of unfractured and cataclastic components suggesting a proto-cataclasite classification[23]. Pyrite crystals range from large (mm) to dust-sized (μm) particles. It is unlikely that this fault acted as a conduit for fluid-flow for sufficient time to allow growth of large pyrite crystals, rather that secondary pyrite cementation occurred following deformation. An outer domain surrounds the pyritised fault gouge. Here cataclastic processes have reduced grain sizes and increased the efficiency of grain packing. Diffusive mass transfer has resulted in enhanced quartz cementation throughout this domain. Pore lining/occluding kaolinite is also present and has been deformed. Pyrite is confined to dilated fault strands, although occasional offshoots from faults are observed. Little post-cementation grain fracturing is noted. The faults are not heavily quartz cemented suggesting most fault activity occurred at shallow depths and temperatures <90ºC. However, cataclasis is observed and the wide grain-size distribution exhibited by these faults suggests more than one phase of deformation.

Capillary pressure measurements on faults in the outer damage zone from Yodel-2 show threshold pressures in the region of 40-80 psi, which, while higher than that of the reservoir (2-4 psi), will not form a significant seal over geological time[21]. However, the inner fault damage zone has threshold pressures of ~8,500 psi and has a water permeability (0.02 mD) six orders of magnitude lower than that of the undeformed reservoir sandstone (10 D). These data indicate a significant seal capacity with the fault capable of baffling hydrocarbon flow on both geological and production timescales.

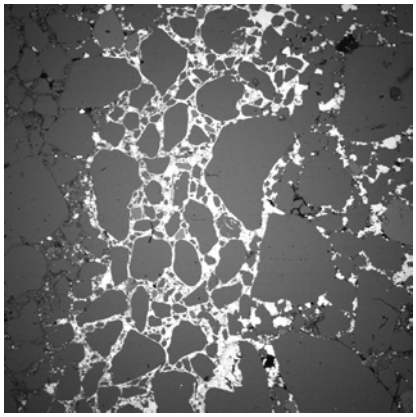

**Figure 4: Backscattered electron micrograph of cemented proto-cataclasite[21] (Yodel-2). Field of view is ~4 mm.**

## Geomechanical results

Cataclasites from Banyula-1 exhibit a lower cohesive strength (5.4 MPa as opposed to 8.8 MPa: Figure 5) but a higher friction coefficient (0.78 as opposed to 0.67) than their associated reservoir. Fault failure envelopes intersect at ~30 MPa, indicating that the cataclasites are more likely to fail at low differential stress while the reservoir sandstone would fail at high differential stress.

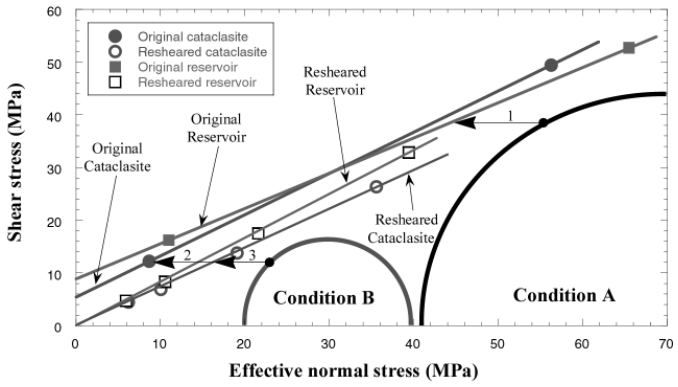


**Figure 5: Intact and reactivated cataclasite and reservoir failure envelops (Banyula-1).**

Jacaranda Ridge-1 reservoir sandstones, cataclasites and phyllosilicate framework faults all have similar failure envelopes (Figure 6). Fault cohesive strength ranges from 12.5-14.8 MPa and friction coefficients are 0.75-0.86. Surprisingly, the clay-rich fault rocks exhibit the greatest cohesive strengths, highest friction coefficient and are stronger than both cataclasite and reservoir rock at all effective normal stresses. Failure envelopes of the cataclasite and reservoir sandstone intersect at effective normal stresses of ~25 MPa. These data suggest that the cataclasite is more likely to fail when differential stress is high, while the reservoir would preferentially fail under low differential stress conditions.

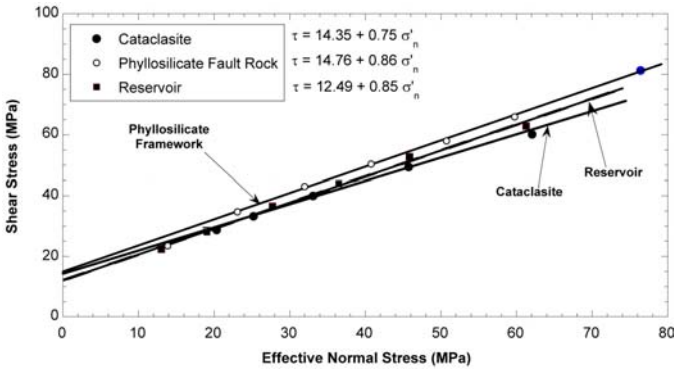


**Figure 6: Cataclasite, phyllosilicate framework fault and reservoir failure envelopes from Jacaranda Ridge-1.**

The principal fault from the Yodel-2 core exhibits cohesive strength of ~17 MPa and friction coefficient of 1.12, well in excess of the outer damage zone faults and reservoir rocks analysed from this well (Figure 7). Outer damage zone faults have failure envelopes that fall in a narrow band with cohesive strengths between 3.76-10.11 MPa and friction coefficients of 0.59-0.87. Hence, the high strength of only the principal slip plane dictates the overall reactivation potential of this fault.

The importance of these geomechanical results is twofold. Firstly they demonstrate that fault rocks can have significant cohesive strength. Secondly, they show that while fault rocks can be weaker than their host reservoir sandstones, as is often assumed, they can also be appreciably stronger as a result of post deformation lithification/cementation. Both these observations have significant implications for the assessment of reactivation potential and associated seal breach through geomechanical methods. Current geomechanical methods for assessing reactivation potential often assume cohesionless fault planes and thus shear failure alone, not allowing for the development of tensile and mixed mode fractures. This may lead to a significant error in assessing reactivation potential and thus fault seal integrity. Equally importantly, most geomechanical analyses implicitly assume that fault rocks are weaker than the reservoir rocks from which they were derived, yet laboratory results and microstructural observations presented herein demonstrate this assumption is not always the case. The two cases of stronger fault rocks presented here both intersect hydrocarbon columns.

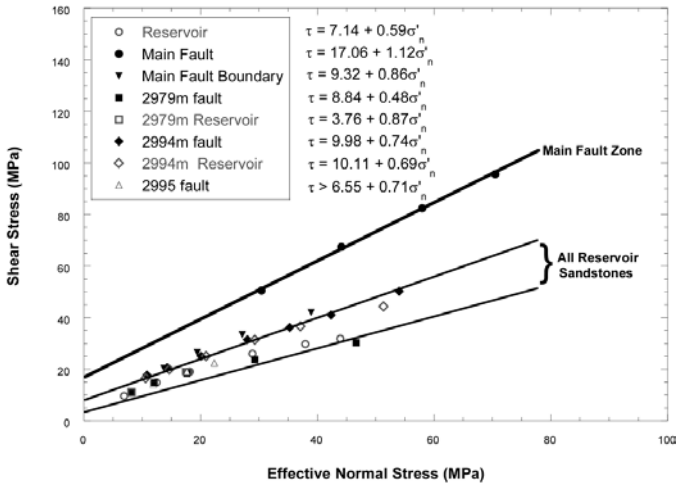


**Figure 7: Principal fault (cataclasite), damage zone faults and reservoir failure envelopes (Yodel-2).**

## Predicting the risk of fault reactivation

The likelihood of fault reactivation and seal breach can be risked via integration of stress field data, fault geometry and the failure envelope for the fault rocks (FAST methodology[11, 33]). Density and check shot velocity data yield the vertical stress, borehole breakouts and drilling-induced tensile fractures yield the orientation of the horizontal stresses, leak-off and extended leak-off tests yield the minimum horizontal stress, and the maximum horizontal stress can be modelled via integration of rock strength data and data noted above using standard industry techniques[24, 25, 26]. Fault azimuth and dip are determined from seismic interpretation. Knowledge of the fault failure envelope is determined from laboratory testing as described above and constitutes a critical difference between the technique presented herein and previous methods[18,19,27,28] for assessing fault reactivation risk.

Given the above information, there are three critical stages to assessing fault reactivation risk (Figure 8):

1. 3-Dimensional (3D) Mohr diagram representing the stress state and failure envelope for the fault is constructed. The risk of reactivation of a plane may be expressed as the increase in pore pressure (ΔP) required to induce fault failure, i.e. horizontal distance on a 3D Mohr diagram between a plane and the failure envelope. The ΔP for all planes may be plotted on a lower hemisphere, normal to plane polar diagram.
2. Fault architecture is mapped and polygons are collapsed to a series of centerline points. Each point along the fault has an associated dip and dip direction.
3. The reactivation risk (ΔP) for each fault segment is mapped on to the fault centerline trace. These data incorporate 3D information in a 2D plane.

The advantages of this methodology are twofold. Realistic failure envelopes derived from laboratory tests can be considered with respect to the in situ stress field and the likelihood of reactivation by all modes of failure can be assessed with a single calculation as opposed to separate slip and dilation tendency analyses [27].

**Strong faults**

Faults can seal by a number of mechanisms including clay smear, cataclasis and cementation. Such processes are directly relevant to the strength of the fault rock products formed in that their ductility and/or lithification state will govern their geomechanical response. In the case of clay smear and cataclasis without post deformation lithification, fault strength will be controlled by the residual strength of the fault rocks and in general, such deformation will be almost cohesionless. However, where significant post deformation cementation has taken place, fault strength is likely to increase, possibly above that of the host reservoir lithology.

Strong faults are defined as faults that fail at higher shear stress than intact reservoir rocks for the same effective normal stress. The strength testing undertaken herein reveals several strong fault classes. The Jacaranda Ridge-1 phyllosilicate framework faults (Figure 6) and the main fault zone from Yodel-2 (Figure 7) are stronger than their respective host reservoir sandstones at all effective normal stress levels. The Jacaranda Ridge-1 cataclasite is stronger than the reservoir sandstone at low effective normal stress yet weaker at normal stresses >25 MPa. The Banyula-1 cataclasite is weaker than the intact reservoir rock at low effective normal stress but stronger at effective normal stresses >30 MPa.

Geomechanical techniques used to predict fault reactivation based on the assumption of zero cohesion are particularly inappropriate in the case of strong faults. Strong faults are unlikely to be reactivated and the seal breach risk is consequently low. Considering the Yodel-2 cemented proto-cataclasite and the Jacaranda Ridge-1 phyllosilicate framework faults, respective reservoir rocks would fail before fault reactivation under all prevailing stress conditions. In such cases, the orientation of the trap-bounding fault is not relevant to assessing reactivation potential. The preservation of hydrocarbon columns at these localities may be related to the fact that the trap-bounding faults are strong and, therefore, not prone to reactivation.

An additional complication in the case of strong fault rocks that needs to be considered is the likelihood of reactivation of the interface between fault and intact rock[32]. Such competency contrast at fault-reservoir boundaries has been observed microstructurally to play a role in cataclasite reactivation[29]. Major faults can develop damage zones many tens of meters from the principal slip plane. Outer damage zone faults typically appear weaker than cemented fault cores. For example, the boundary between fault core and reservoir in Yodel-2 is weaker than the main fault zone, while damage zone faults and intact reservoir sandstones tend to have similar geomechanical properties (Figure 7).

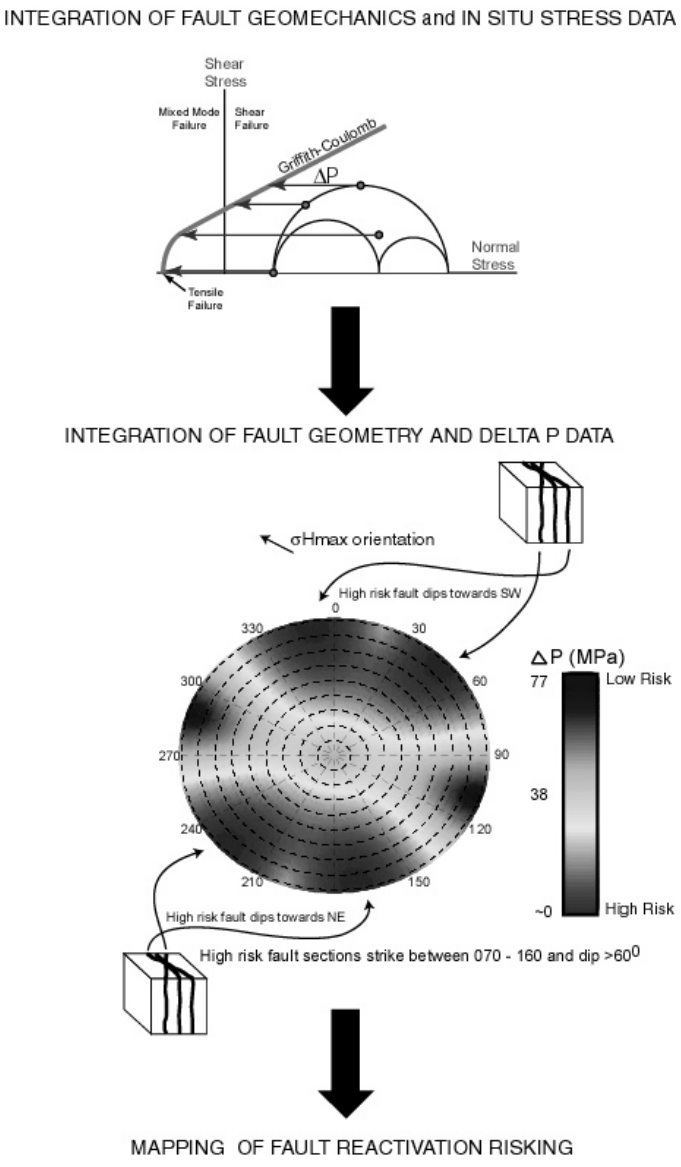


**Figure 8: Integration of geomechanics and stress data to model risk of fault seal reactivation (see text for details).**

The enhancement of fault strength through cementation can result in the development of considerable cohesive and, therefore, tensile strength so facilitating the possibility of shear, tensile and mixed-mode failure. Where tensile strength exists, tensile failure can occur under low differential stress conditions ($\sigma_1$-$\sigma_3$ < 4T), while mixed mode extensional shear fractures form at differential stresses intermediate to tensile and shear failure (4T-6T) using a Griffith-Coulomb failure envelope. In general, many instances of fracture-induced top seal failure have been ascribed to tensile failure as a result of pore pressure reducing the minimum effective stress beneath rock tensile strength [4, 32]. However, in fault zones, reactivation in tension can only occur when faults have become severely misoriented for shear reactivation with respect to the stress field or when such faults have regained cohesive strength due

to cementation[22, 31]. Data presented herein confirm that faults are not always cohesionless or weak and may be considerably stronger than their undeformed host rocks.

### Application of geomechanics to fault seal risking

Due to the lack of published geomechanical data, fault failure envelopes are typically estimated from data collated by Byerlee[20] resulting in friction coefficients on the order of ~0.60 and 0 MPa cohesive strength. The use of Byerlee-derived failure envelopes only allows for shear failure conditions to be considered. Closer examination of the data and theory presented by Byerlee[20] shows that while an approximation that ignores cohesive strength makes little difference at high effective normal stresses (>100 MPa), the lower the effective normal stress, the greater the error induced by neglecting cohesive strength. It is likely that fault rocks in petroleum systems at depths of 1-4 km fall in the lower effective stress window.

The impact of risking fault sealed traps using laboratory-derived geomechanical data verses Byerlee[20] data is demonstrated below. Two cases are considered: Scenario 1 where the probability of fault rock process sealing *(a)* and juxtaposition sealing *(b)* are 0.8 and 0.9 respectively, and where fault reactivation is risked via the ΔP methodology (see Figure 8) using Byerlee data of $\mu = 0.6$, $C_o = 0$ MPa, $T = 0$ MPa. Scenario 2 considers the case where the probability of fault rock process sealing and juxtaposition sealing and remain 0.8 and 0.9 respectively, yet where fault reactivation is risked using geomechanics data derived from laboratory investigation of Jacaranda Ridge-1 phyllosilicate framework fault ($\mu = 0.86$, $Co = 14.76$ MPa, $T = 7.38$ MPa). The high seal condition values ascribed to both examples would represent the scenario where faulting has maintained reservoir - non-reservoir juxtaposition, and modeled SGR values are >0.7 (high probability of fault plane process seal, i.e. clay smear). A pore pressure of 28 MPa was applied in both cases (hydrostatic regime).

The probability of a fault seal being developed (FSD) in Scenario 1 can be expressed by:

$$FSD = \{1 - [( 1 - 0.8 )( 1 - 0.9 ) ] \} = 0.98$$

This figure represents only the probability that a seal has developed. It does not integrate the likelihood that the fault seal may have been reactivated and breached by structural permeability networks. The probability of the fault remaining unbreached with respect to the present day principal stress state and pore-pressure conditions is calculated via the FAST methodology (Figure 8). The minimum ΔP for Scenario 1 fault reactivation is calculated as ~1 MPa. Given the extremely low additional pressure required to induce fault seal failure, a reactivation risk value for this fault is 0.9 (extremely likely that the seal is breached, see Figure 2). The integrated fault seal probability (FS) for Scenario 1 can be expressed as:

$$FS = \{1 - [( 1 - 0.8 )( 1 - 0.9 ) ] \} \times ( 1 - 0.9 ) = 0.1$$

A fault seal condition of 0.1 (seal condition is extremely unlikely) would result in a very high prospect risk when all other factors required for hydrocarbon trapping (i.e. charge, trap formation, migration pathway) are considered. Unless the expected net present value (ENPV) was sufficiently large, i.e. the potential prize outweighs the high risk for trap breach, it is highly unlikely that this prospect would be drilled.

The probability of a fault seal being developed (FSD) in Scenario 2 remains 0.98 (seal condition extremely likely). However, the probability of the fault remaining unbreached within the present day stress regime now utilizes intact fault geomechanical data. Using the FAST methodology, the minimum ΔP for Scenario 2 fault is calculated as ~28 MPa. Given the high ΔP required to push the fault to failure, a seal risk condition of 0.2 is applied (seal very unlikely to be reactivated under present day stress and pore pressure conditions). The integrated fault seal probability (FS) for Scenario 2 can now be expressed as:

$$FS = \{1 - [( 1 - 0.8 )( 1 - 0.9 ) ] \} \times ( 1 - 0.2 ) = 0.78$$

Comparison of the integrated fault seal probability for Scenarios 1 and 2 reveal a marked decrease in prospect structural risk simply through application of geomechanical fault data. Geological conditions remain constant between both scenarios however, the reduced risk of reactivation in Scenario 2 dictates the integrated fault seal risk to be significantly diminished. Other factors being favorable, such a high probability of fault sealing in Scenario 2 would provide a strong case for drilling the prospect.

## CONCLUSIONS

Cataclastic faults, disaggregation zones and phyllosilicate framework fault rocks analysed from the Carnarvon and Otway Basins exhibit significant post-deformation lithification due to quartz and/or pyrite cementation that has resulted in the regaining of cohesive and tensile strength. Such fault healing allows the development of tensile, shear and mixed mode fractures during reactivation. The geomechanical properties of fault rocks govern their response to imposed stress fields and, therefore, significantly affect fault zone strength and reactivation potential. Evaluation of fault seal risk needs to consider not only the potential for seal development, but also the likelihood that the seal remains unreactivated.

Fault seal reactivation risking can be undertaken using a geomechanical approach. Current techniques tend to assume faults are cohesionless and apply a simple friction law to derive a failure envelope. While geomechanical techniques that assess reactivation based only on shear failure are not incorrect, methodologies that do not account for enhanced fault strength are likely to erroneously estimate the reactivation seal risk due to dismissal of tensile failure. The impact of structurally risking traps using Byerlee and laboratory-derived fault data has been demonstrated using the Fault Seal Risk Web approach. In the case of strong faults, application of geomechanical fault data results in a significant

decrease in prospect structural risk due to consideration of fault gouge cohesive and tensile strength during reactivation modeling.

Where limited data are available for conducting geomechanical fault analysis, it is recommended that sensitivity analyses be undertaken to determine the effects of both varying friction angle and increased cohesive strength along fault zones where seal breach due to reactivation is perceived as the major prospect risk. Future fault seal reactivation research needs to focus not only on geomechanical techniques for predicting the likelihood of reactivation of weak faults, but also on the prediction of failure envelopes and whether trap-bounding faults are likely to be stronger than intact reservoir rock. This would incorporate the prediction of both physical fault rock-forming processes and subsequent diagenetic modification.

## REFERENCES


1. Rose, P.R: "Chance of success and its use in petroleum exploration" In: Steinmetz, J. (Ed.) *The Business of Petroleum Exploration*, *AAPG Treatise of Petroleum Geology,* (1992) 71.
2. Otis, R.M. and Schneidermann, N.: "A process for evaluating exploration prospects" *AAPG Bulletin,* **81**, (1997), 1087.
3. Watson, P.: "A process for estimating geological risk of petroleum exploration prospects" *Australian Petroleum Production and Exploration Association Journal*, **38**, (1998), 577.
4. Watts, N. L.: "Theoretical aspects of cap-rock and fault seals for two-phase hydrocarbon columns" *Marine and Petroleum Geology*, **4** (1987), 274.
5. Allan, U.S.: "Model for hydrocarbon migration and entrapment within faulted structures" *AAPG Bulletin*, **73**, (1989), 803.
6. Freeman, B., Yielding, G. and Badley, M.: "Fault Correlation During Seismic Interpretation" *First Break*, **8**, (1990), 3.
7. Yielding, G., Freeman, B. and Needham, D. T.: "Quantitative fault seal prediction" *AAPG Bulletin*, **81**, (1997), 897.
8. Antonellini, M. and Aydin, A.: "Effect of faulting on fluid flow in porous sandstones: petrophysical properties" *AAPG Bulletin*, **78**, (1994), 355.
9. Knipe, R. J.: "Faulting process and fault seal". In: Larson, R. M., Breke, H., Larsen B. T., and Talleraas, E. (Eds.). *Structural and Tectonic Modeling and it's Application to Petroleum Geology*. NPF Special Publication 1, Stavanger, (1992), 325.
10. Bouvier, J. D., Sijpesteijn, K., Kleusner, D. F., Onyejekwe, C. C. and Van der Pal, R. C.: "Three Dimensional Seismic Interpretation and Fault Sealing Investigations, Nun River, Nigeria" *AAPG Bulletin*, **73**, (1989), 1397.
11. Jones, R. M., Boult, P., Hillis, R. R., Mildren S. D. and Kaldi, J: "Integrated Hydrocarbon Seal Evaluation in the Penola Trough, Otway Basin" *Australian Petroleum Production and Exploration Association Journal,* **40**, (2000), 194.
12. Grauls, D. J. and Baleix, J. M.: "Role of overpressures and *in situ* stresses in fault-controlled hydrocarbon migration: a case study" *Marine and Petroleum Geology*, **11**, (1994), 734.
13. Shuster, M. W., Eaton, S., Wakefield, L. L. and Kloosterman, H. J.: "Neogene tectonics, greater Timor Sea area, offshore Australia: implications for trap risk" *Australian Petroleum Production and Exploration Association Journal*, **38**, (1998), 351.
14. Jones, R. M. and Hillis, R. R. "An Integrated, Quantitative Approach to Assessing Fault Seal Risk" paper presented at 2000 AAPG Conference, Bali, Sept.
15. Jones, R. M. and Hillis, R. R. "An Integrated, Quantitative Approach to Assessing Fault Seal Risk" *Shell EPNL,* **December**, (2001), 7.
16. Sibson, R. H.: "Implications of fault-valve behavior for rupture nucleation and occurrence" Tectonophysics, **211**, (1992), 283.
17. Barton, C. A., Zoback, M. D. and Moos, D.: "Fluid flow along potentially active faults in crystalline rock" *Geology*, **23**, (1995), 683.
18. Morris, A., Ferrill, D. A. and Henderson, D. B.: "Slip-tendency analysis and fault reactivation" *Geology*, **24**, (1996), 275.
19. Castillo, D. A., Bishop, D. J., Donaldson, I., Kuek, D., De Ruig, M. J., Trupp, M. and Schuster, M. W.: "Trap integrity in the Laminaria High-Nancar Trough region, Timor Sea: prediction of fault seal failure" *Australian Petroleum Production and Exploration Association Journal*, **40**, (2000), 151.
20. Byerlee, J. D.: "Friction of rocks" *Pure and Applied Geophysics,* **116**, (1978), 615.
21. Dewhurst, D.N., Jones, R.M., Hillis, R.R. & Mildren, S.D., "Microstructural and Geomechanical Characterisation of Fault Rocks from the Carnarvon and Otway Basins". *Australian Petroleum Production and Exploration Association Journal*, **42**, (2002), 167.
22. Sibson, R. H.: "Structural permeability of fluid-driven fault fracture meshes" *Journal of Structural Geology*, **18**, (1996), 1031.
23. Fisher, Q. J. and Knipe, R. J.: "Fault sealing processes in siliciclastic sediments". In: Jones, G., Fisher, Q.J., and Knipe, R. J., (Eds.), *Faulting, fault sealing and fluid flow in hydrocarbon reservoirs. Geological Society of London, Special Publication*, **147**, (1998), 117.
24. Bell, J. S.: "The stress regime of the Scotian Shelf offshore eastern Canada to 6 kilometers depth and implications for rock mechanics and hydrocarbon migration" In: Maury, V. and Fourmaintraux, D. (Eds.), *Rock at Great Depth*, **3**, 1243.
25. Moos, D. and Zoback, M. D.: "Utilization of observations of well bore failure to constrain the orientation and magnitude of crustal stresses" *Journal of Geophysical Research*, **95**, (1990), 9305.
26. Hillis, R. R. and Reynolds, S. D.: "The Australian stress map" *Journal of the Geological Society of London*, **157**, (2000), 915.
27. Ferrill, D. A., Winterle, J., Wittmeyer, G., Sims, D., Colton, S., Armstrong, A. and Morris, A. P.: "Stressed rock strains groundwater at Yucca Mountain, Nevada" *GSA Today*, **9**, (1999), 1.
28. Wiprut, D. and Zoback, M. D.: "Fault reactivation and fluid flow along a previously dormant normal fault in the northern North Sea" *Geology*, **28**, (2000), 595.
29. Dewhurst, D. N. and Jones, R. M.: "Geomechanical, microstructural and petrophysical evolution in experimentally reactivated cataclasites: application to fault seal prediction" *AAPG Bulletin*, in press, August, 2002.
30. Caillet, G.: "The caprock of the Snorre Field, Norway: A possible leakage by hydraulic fracturing" *Marine and Petroleum Geology*, **10**, (1993), 42.
31. Sibson, R. H.: "Conditions for rapid large-volume flow" In Arehart, G. B. and Hulston, J. R (Eds.), Water-Rock Interaction: *Proceedings of the 9th International Symposium*, (1998), 35.
32. Streit, J. E.: "Conditions for earthquake surface rupture along the San Andreas fault system, California" *Journal of Geophysical Research*, **104**, (1999), 17929.
33. Mildren, S.D., Hillis, R.R. and Kaldi, J. Calibrating predictions of fault seal reactivation in the Timor Sea. *Australian Petroleum Production and Exploration Association Journal*, **42**, (2002), 187.